

Amorphous indium-gallium-zinc-oxide visible-light phototransistor with a polymeric light absorption layer

Hsiao-Wen Zan, Wei-Tsung Chen, Hsiu-Wen Hsueh, Shih-Chin Kao, Ming-Che Ku, Chuang-Chuang Tsai, and Hsin-Fei Meng

Citation: *Applied Physics Letters* **97**, 203506 (2010); doi: 10.1063/1.3517506

View online: <http://dx.doi.org/10.1063/1.3517506>

View Table of Contents: <http://scitation.aip.org/content/aip/journal/apl/97/20?ver=pdfcov>

Published by the [AIP Publishing](#)

Articles you may be interested in

[Reduction of defect formation in amorphous indium-gallium-zinc-oxide thin film transistors by N₂O plasma treatment](#)

J. Appl. Phys. **114**, 204501 (2013); 10.1063/1.4832327

[High responsivity of amorphous indium gallium zinc oxide phototransistor with Ta₂O₅ gate dielectric](#)

Appl. Phys. Lett. **101**, 261112 (2012); 10.1063/1.4773307

[Room-temperature-operated sensitive hybrid gas sensor based on amorphous indium gallium zinc oxide thin-film transistors](#)

Appl. Phys. Lett. **98**, 253503 (2011); 10.1063/1.3601488

[Environment-dependent thermal instability of sol-gel derived amorphous indium-gallium-zinc-oxide thin film transistors](#)

Appl. Phys. Lett. **98**, 152109 (2011); 10.1063/1.3580614

[Light induced instabilities in amorphous indium-gallium-zinc-oxide thin-film transistors](#)

Appl. Phys. Lett. **97**, 173506 (2010); 10.1063/1.3503971



NEW! Asylum Research MFP-3D Infinity™ AFM
Unmatched Performance, Versatility and Support

OXFORD INSTRUMENTS
The Business of Science®

Stunning high performance
Simpler than ever to GetStarted™

Comprehensive tools for nanomechanics
Widest range of accessories for materials science and bioscience

Amorphous indium-gallium-zinc-oxide visible-light phototransistor with a polymeric light absorption layer

Hsiao-Wen Zan,^{1,a)} Wei-Tsung Chen,¹ Hsiu-Wen Hsueh,¹ Shih-Chin Kao,¹ Ming-Che Ku,¹ Chuang-Chuang Tsai,¹ and Hsin-Fei Meng²

¹Department of Photonics and Institute of Electro-Optical Engineering, National Chiao Tung University, 1001, Ta Hsueh Road, Hsinchu 300, Taiwan

²Institute of Physics, National Chiao Tung University, 1001, Ta Hsueh Road, Hsinchu 300, Taiwan

(Received 30 May 2010; accepted 28 October 2010; published online 18 November 2010)

This work demonstrates a real-time visible-light phototransistor comprised of a wide-band-gap amorphous indium-gallium-zinc-oxide (*a*-IGZO) thin-film transistor (TFT) and a narrow-band-gap polymeric capping layer. The capping layer and the IGZO layer form a *p-n* junction diode. The *p-n* junction absorbs visible light and consequently injects electrons into the IGZO layer, which in turn affects the body voltage as well as the threshold voltage of *a*-IGZO TFT. The hysteresis behavior due to the charges at IGZO back interface is also discussed. © 2010 American Institute of Physics. [doi:10.1063/1.3517506]

Thin-film transistors with amorphous metal oxide films, such as zinc oxide and amorphous indium-gallium-zinc-oxide (*a*-IGZO) films, have attracted considerable attention owing to their potential applications to flat, flexible, and transparent display devices.^{1,2} At present, considerable research efforts are being devoted to the development of touch-screen technology by integrating photosensors into display panels. Attempts to develop a sensitive *a*-IGZO phototransistor on the basis of the standard *a*-IGZO thin-film transistor (TFT) fabrication process are underway. Amorphous metal oxides have a large energy band gap (more than 3 eV), and therefore, metal-oxide TFTs exhibit a low response to light with wavelengths (λ) greater than 420 nm (i.e., photon energy lower than 2.95 eV).³ It has been reported that the threshold voltage of metal-oxide TFTs decreases under visible light illumination. However, it eventually recovers owing to the persistent photoconductivity effect, exhibiting a time constant of 20 h.⁴

In this paper, we propose a simple method of converting a wide-band-gap metal-oxide TFT into a visible light phototransistor that has a high sensitivity and a fast response. After capping a polymer semiconductor film having a high absorption coefficient for visible light, i.e., poly(3-hexylthiophene) (P3HT), onto a conventional top-contact bottom-gate *a*-IGZO TFT, significant photocurrent was observed under visible light illumination. The photocurrent is found to be dominated by a fast-shifted threshold voltage. A mechanism considering exciton separation, electron accumulation, and back channel effect is proposed and discussed.

A 100-nm-thick thermal silicon nitride (SiN_x) layer is grown on heavily doped Si wafers to serve as the gate dielectric. A 50-nm-thick *a*-IGZO (3 in. circular target; In:Ga:Zn=1:1:1 at. %) layer is deposited by radio-frequency (rf) sputtering onto the thermally grown SiN_x layer through a shadow mask to form the active layer at room temperature. The rf power and pressure are maintained at 70 W and 7 mTorr, respectively; the Ar flow rate is maintained at 30 SCCM (SCCM denotes cubic centimeter per minute at

STP). A 50-nm-thick Al layer is deposited through a shadow mask to form the source and drain contacts. The annealing process is carried out at 350 °C in a nitrogen furnace for 1 h. Then, P3HT derived from chlorobenzene (2.5 wt %) is coated on some of the devices; the coated devices are then annealed at 200 °C for 10 min. The thickness of the P3HT film is 100 nm. The schematic cross-sectional diagram of a device without P3HT capping [i.e., a standard (STD) device] is shown in Fig. 1(a). The schematic cross-sectional diagram of a P3HT-capped device is shown in Fig. 1(b). The device channel length (L) and channel width (W) are fixed at 300 and 1000 μm , respectively. The white light source is an light-emitting diode backlight, such as the ones used in liquid crystal displays (LCD) with a power density of 1.2 mW/cm^2 ; it irradiates the sample from the top. The threshold voltage and mobility were determined from the slope and the x -axis intercept of the $\sqrt{I_D}$ - V_G curve measured under saturation condition ($V_{DS}=20$ V; V_{GS} was varied from -15 to 20 V).

Figure 1(c) shows the absorption coefficient spectra of P3HT and *a*-IGZO films. The *a*-IGZO layer is apparently blind to visible light, whereas the P3HT layer absorbs visible

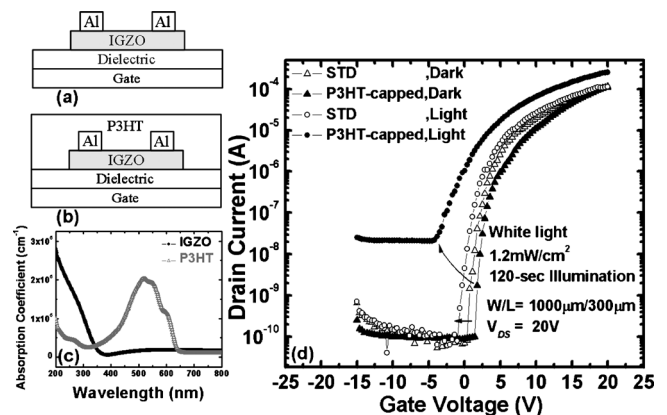


FIG. 1. (a) Schematic diagram of STD device, (b) schematic diagram of P3HT-capped *a*-IGZO TFT, (c) absorption coefficient spectra of *a*-IGZO and P3HT thin films, and (d) transfer characteristics before and after 120 s white light illumination of STD device and P3HT-capped *a*-IGZO TFT.

^{a)}Author to whom correspondence should be addressed. Electronic mail: hsiaowen@mail.nctu.edu.tw.

light well. The transfer characteristics of the P3HT-capped *a*-IGZO TFT device and the STD device before and after 120 s illumination are compared in Fig. 1(d). In the dark, the STD and the P3HT-capped devices exhibit similar transfer characteristics. Though P3HT is a *p*-channel material, P3HT-capped device is not an ambipolar device because P3HT, with a band gap around 2 eV, has a very low intrinsic hole concentration. Holes in P3HT are mostly injected from source and drain metals. Since the highest occupied molecular orbital (HOMO) level of P3HT is as high as 5 eV, aluminum (the source/drain metal in this work) with work function around 4.3 eV is not able to inject holes into P3HT efficiently. The threshold voltage (V_{th}), mobility (μ), and subthreshold swing of the P3HT-capped *a*-IGZO TFT were determined to be 2.3 V, 10.8 cm²/V s, and 0.34 V/decade, respectively. Those of the STD device were 2.1 V, 7.55 cm²/V s, and 0.42 V/decade, respectively. V_{th} of P3HT-capped *a*-IGZO TFT is slightly more positive than that of STD device. This is because that, to form P3HT/IGZO *p-n* junction, holes diffuse from P3HT into IGZO back interface to reach thermal equilibrium. The positive charges at IGZO back interface make V_{th} shift to be more positive. Hysteresis behavior associated with the holes at IGZO back interface will be discussed later. Under illumination, the P3HT-capped *a*-IGZO TFT exhibits a greater photoresponse as compared to the STD device. In the case of the P3HT-capped device, the off-state and on-state currents are clearly elevated. ΔV_{TH} is greater than 6 V after 120 s white light illumination. It is known that, under illumination, excitons are generated inside the P3HT layer. Owing to their high binding energy, the excitons undergo dissociation only at the P3HT/IGZO interface. After exciton dissociation, electrons enter the IGZO film leaving behind holes in the P3HT film. With a drain-to-source bias, photoinduced carriers flow to the source/drain electrodes, generating an off-state photocurrent. Photocurrent (I_{ph}) is calculated as the drain current under illumination minus the drain current in the dark. In Fig. 1(d), an off-state I_{ph} of about 30 nA is observed. At a fixed gate bias such as $V_G=15$ V, the on-state I_{ph} is 60 μ A. The above mechanism is not able to explain the on-state I_{ph} considering that it is almost 2000 times greater than the off-state I_{ph} . When we change the *x*-axis parameter in Fig. 1(d) from V_{GS} to $V_{GS}-V_{TH}$ in order to exclude the influence of light-induced ΔV_{TH} , the on-state currents before and after illumination are almost identical. It can thus be concluded that the high on-state I_{ph} for the P3HT-capped device is due to the significant light-induced ΔV_{TH} .

In Fig. 2(a), ΔV_{TH} values of the STD and the P3HT-capped devices are plotted as a function of the illumination time. The P3HT-capped device exhibits rapid and substantial threshold voltage drop during white light illumination. The photoresponsivity (R_{ph}) of the STD and the P3HT-capped devices as a function of gate bias are also plotted in Fig. 2(b). R_{ph} is defined as $I_{ph}/(EWL)$, where E is the power intensity of incident light (in W/cm²). Measurements were taken after 20 and 120 s white light illumination periods with light intensity maintained at 1.2 mW/cm². R_{ph} goes as high as 4 A/W at $V_{GS}=15$ V after a 20 s illumination. In contrast, STD device exhibits low R_{ph} .

After discontinuing the illumination, ΔV_{TH} was studied by measuring its variation in response to current generated under pulsed illumination. As mentioned before, on-state I_{ph}

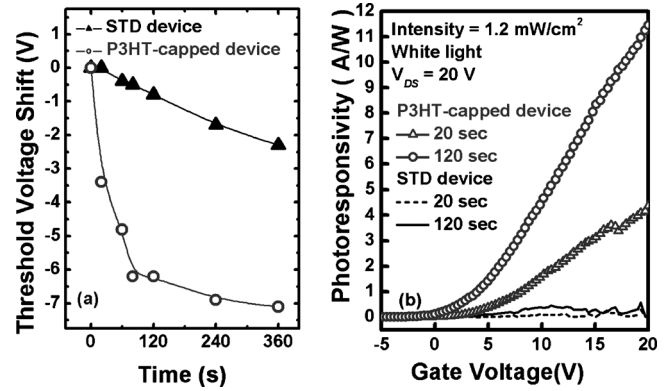


FIG. 2. (a) The threshold voltage shift as a function of illumination time and (b) the photoresponsivity as a function of gate bias of STD and P3HT-capped *a*-IGZO TFT.

is dominated by ΔV_{TH} . A white light source pulsing at a frequency of 1 Hz was used. Drain currents of both the P3HT-capped and the STD devices in the turn-on condition were tracked as shown in Fig. 3. When $V_{DS}=20$ V and $V_{GS}=15$ V, the STD device shows no response to pulsed illumination. The fact that the STD device exhibits response to continuous irradiation [as shown in Fig. 2(a)] but has no response to pulsed illumination (as shown in Fig. 3) reveals that the photoresponse in STD device is slow. The slow photoresponse in metal-oxide phototransistor was reported to be attributed to the persistent photoconductivity effect in the metal oxide thin film. It was proposed that the oxygen adsorbates that become charged by photogenerated carriers affected the energy band bending of the active layer and influenced the device threshold voltage.⁴

For a P3HT-capped device biased with $V_{GS}-V_{TH}=9$ V as shown in Fig. 3, rapid and significant current response is obtained in the saturation region ($V_{DS}=20$ and 10 V). In the linear region, small response is obtained when $V_{DS}=5$ V and

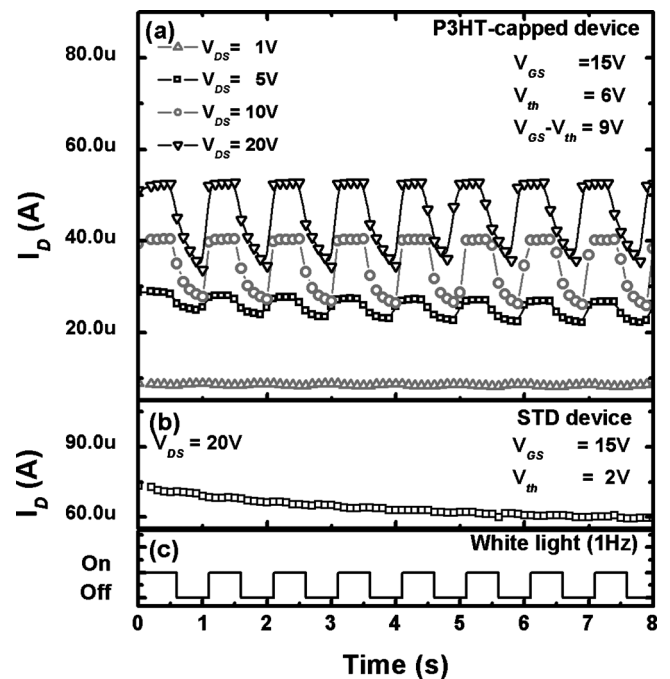


FIG. 3. On currents of P3HT-capped and STD devices monitored under pulsed illumination of 1 Hz frequency.

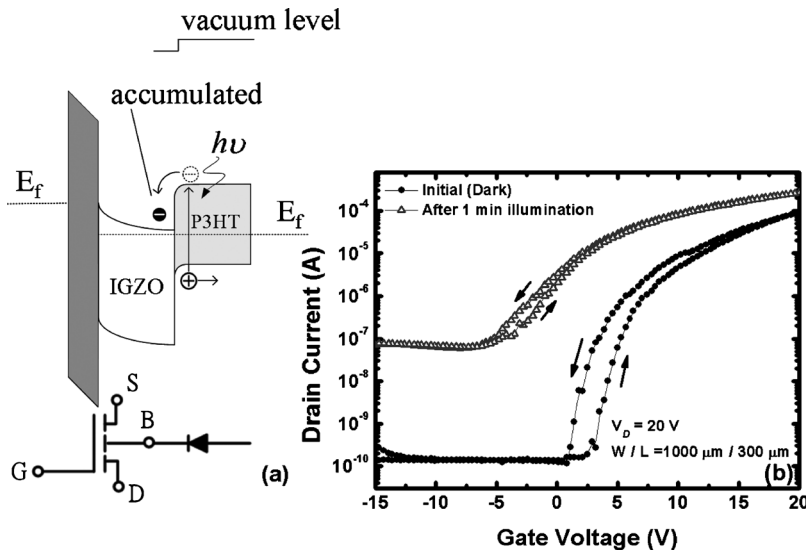


FIG. 4. (a) Schematic energy-band diagram of the P3HT-capped *a*-IGZO TFT near the drain side when device is operated in saturation mode. (b) Hysteresis behavior for a P3HT-capped IGZO TFT in dark and under illumination.

no response is observed when $V_{DS}=1$ V. We attributed the P3HT capping-effect to the rapid fluctuations in electron concentration in the back channel region. As shown in the energy band diagram in Fig. 4(a), when an IGZO TFT is operated in the saturation condition, the energy band in the IGZO film near the drain side bends down toward the P3HT film to enable the accumulation of light-induced electrons. Electrons accumulated in the back channel region make the device threshold voltage shift left. After removing the light illumination, electrons accumulated at the IGZO/P3HT interface recombine with the holes inside the P3HT film rapidly. Hence, ΔV_{TH} recovers quickly. For a P3HT-capped device in the linear region, the photoresponsivity is poor since the energy band in the IGZO film bends down toward the dielectric to dissipate the electrons away from the back channel region.

To further investigate the influence of charges at back interface, hysteresis behaviors of P3HT-capped device in dark and under illumination are observed in Fig. 4(b). In dark, P3HT-capped device exhibit obvious hysteresis behavior while STD device has no hysteresis characteristics (not shown). As aforementioned, P3HT/IGZO forms a *p-n* junction and holes in P3HT diffuse into IGZO to reach thermal equilibrium. Holes located at IGZO back interface make P3HT-capped device has a more positive V_{th} than STD device as shown in Fig. 1(d). In *a*-IGZO, holes are easily trapped.⁵ In Fig. 4(b), when gate bias increases to be more positive, reversely biased P3HT/IGZO *p-n* junction causes more holes diffuse into IGZO film. When gate bias starts to decrease and becomes less positive, the holes trapped at IGZO back interface are slowly released from trap states and thus cause hysteresis. Under illumination, hysteresis phenomenon becomes less significant. Photogenerated electrons accumulated in IGZO back channel may speed up the releasing of trapped holes from trapped states and thus suppress the hysteresis effect.

The photodetection mechanism of the P3HT-capped IGZO TFT can be summarized as follows. First, a *p*-type P3HT capping layer is employed as the light absorption layer. Second, energy gap between the HOMO level of P3HT and the conduction band of IGZO is larger than the exciton

binding energy (~ 0.3 eV) so that excitons can be dissociated at P3HT/IGZO interface. Third, the built-in electric field at the P3HT/IGZO *p-n* junction enables the injection of electrons into IGZO film. According to previous reports, the interface between *p*-type P3HT and *n*-type IGZO exhibits a vacuum level difference of 0.3–0.5 eV.^{6–8} The vacuum level difference produces a built-in electric field at the P3HT/IGZO interface that is directed from IGZO to P3HT to enable the injection of electrons into the IGZO film. Finally, the transistor is operated in the saturation region so that the injected electrons accumulate in the back channel in the IGZO layer, resulting in a threshold voltage shift due to the body effect. The body voltage as well as the threshold voltage are sensitive to the amount of accumulated electrons and hence exhibit a fast-switching behavior under pulsed light illumination. This study proposes a significant body effect in IGZO TFT and utilizes the effect to produce a real-time and sensitive visible-light phototransistor. It is expected that the sensing behavior is not limited to photosensing. One can extend the principle to produce various kinds of sensors if the sensing targets react with IGZO back interface to cause a charge transfer and to change the body voltage.

This work was funded through the National Science Council (NSC 99-2628-E-009-010).

- J. S. Park, T. W. Kim, D. Stryakhilev, J. S. Lee, S. G. An, Y. S. Pyo, D. B. Lee, Y. G. Mo, D. U. Jin, and H. K. Chung, *Appl. Phys. Lett.* **95**, 013503 (2009).
- J. Y. Kwon, K. S. Son, J. S. Jung, T. S. Kim, M. K. Ryu, K. B. Park, B. W. Yoo, J. W. Kim, Y. G. Lee, K. C. Park, S. Y. Lee, and J. M. Kim, *IEEE Electron Device Lett.* **29**, 1309 (2008).
- D. P. Gosain and T. Tanaka, *Jpn. J. Appl. Phys., Part 1* **48**, 03B018 (2009).
- P. Görrn, M. Lehnhardt, T. Riedl, and W. Kowalsky, *Appl. Phys. Lett.* **91**, 193504 (2007).
- B. Ryu, H. K. Noh, E. A. Choi, and K. J. Chang, *Appl. Phys. Lett.* **97**, 022108 (2010).
- T. Kamiya, S. Narushima, H. Mizoguchi, K. Shimizu, K. Ueda, H. Ohta, M. Hirano, and H. Hosono, *Adv. Funct. Mater.* **15**, 968 (2005).
- A. J. Cascio, J. E. Lyon, M. M. Beerbom, R. Schlafra, Y. Zhu, and S. A. Jenekhe, *Appl. Phys. Lett.* **88**, 062104 (2006).
- Y. D. Park, J. H. Cho, D. H. Kim, Y. Jang, H. S. Lee, K. Ihm, T. H. Kang, and K. Choc, *Electrochem. Solid-State Lett.* **9**, G317 (2006).